U.S. DEPARTMENT OF ENERGY | Office of Science

DOE/SC-CM-22-002

FY 2022 Second Quarter Performance Metric: Demonstrate Improved Representation of Ocean and Sea Ice Processes Including Arctic-Subarctic Oceanic Exchanges and Sea Ice Thickness Distribution Using Ocean and Sea Ice Regionally Refined Mesh (RRM) Capabilities

April 2022

DISCLAIMER

Contents

Figures

1.0 Product Definition

This report summarizes the progress that has been made to improve the representation of ocean and sea ice processes, including Arctic-Subarctic oceanic exchanges and sea ice thickness distribution, using the Department of Energy's (DOE) Energy Exascale Earth System Model (E3SM) Regionally Refined Modeling (RRM) capabilities for the ocean and sea ice (OSI) model components. To that end, we present the results of simulations with an ocean/sea ice configuration of E3SM with regional grid refinement in the Arctic. This configuration, referred to as E3SM-Arctic-OSI (or E3SM-Arctic for short), has been developed by the HiLAT-RASM project in collaboration with E3SM team members. The grids of the ocean and sea ice components of E3SM-Arctic have a high spatial resolution (10 km) in the Arctic and subpolar North Atlantic Oceans and standard resolution (up to 60 km) elsewhere. The impacts of Arctic Ocean mesoscale are likely not fully accounted for in coarse resolution (i.e., > 25-km) models since the Rossby radius of deformation, required to resolve the ocean mesoscale (e.g., eddies, coastal currents and jets, exchanges through narrow gateways), is on the order of 10 km or less (Nurser and Bacon 2014). This motivated the development of E3SM-Arctic to enable a more realistic representation of Arctic-Subarctic oceanic exchanges and sea ice thickness.

In the next section, we describe the details of this configuration, followed by results that compare the performance of E3SM-Arctic in several key metrics against the standard resolution configuration of E3SM, referred to as E3SM-LR-OSI (E3SM-LR for short; Petersen et al. 2019). The results presented here are primarily based on version 1 of E3SM (Golaz et al. 2019) and have been documented in Veneziani et al. (in press). We will also present some preliminary results from E3SMv2. Our results demonstrate that the Arctic-refined configuration of E3SM provides significant improvements in the representation of features that are important for the Arctic Ocean and its interactions with lower latitudes. These improvements include the strength of the Atlantic Meridional Overturning Circulation (AMOC), ocean heat transport into the Arctic, the stratification of the Arctic, and sea ice deformation. No improvement is found in sea ice thickness distributions, which are controlled primarily by atmospheric forcing. We anticipate seeing more significant improvements in the fully-coupled simulations, where ocean-atmosphere-sea ice interactions can amplify the differences imposed by the more detailed representation of the ice pack (for instance, leads).

2.0 Product Documentation

The ocean and sea ice models of E3SM-Arctic use grids that have a high spatial resolution (10 km) in the Arctic and subpolar North Atlantic Oceans and standard resolution (up to 60 km) elsewhere. Figure 1 shows the resolution as a function of latitude used for E3SM-Arctic (red curves) and E3SM-LR (black). Both configurations have a comparable resolution in the southern hemisphere, with grid sizes ranging from 60 km at southern mid-latitudes to 30 km approaching the south pole and the equator. While E3SM-LR repeats this resolution structure in the northern hemisphere, the resolution in E3SM-Arctic transitions from 30 km at the equator to 10 km at the North Pole. In order to ensure that the exchanges between the North Atlantic and Arctic are accurately represented, the transition towards high resolution starts at lower latitudes (10°) in the Atlantic than in the Pacific (30°).

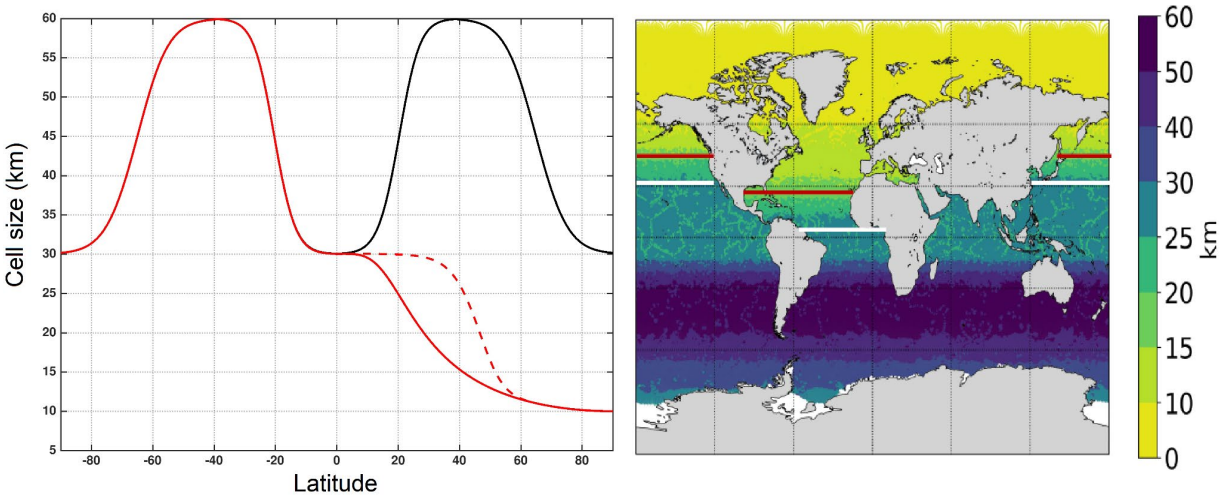

Figure 1. *Left: Distribution function for cell size as a function of latitude. The black curve indicates the E3SM-LR mesh, while the red curves indicate the E3SM-Arctic mesh. The solid and dashed red lines mark resolution changes in the Atlantic and Pacific Oceans, respectively. The resolution in the Southern Ocean is the same for E3SM-Arctic and E3SM-LR. Right: Geographical distribution of grid cell size for the E3SM-Arctic configuration. The area between the white and red lines denotes the region where the GM parameterization transitions from on to off.*

Figure 2 shows how E3SM-Arctic resolves the main narrow gateways in and out of the Arctic Ocean, which are not realistically represented in E3SM-LR. These passages have been shown to play an important role in the exchange of heat and freshwater between the Subpolar North Atlantic/Pacific and the Arctic Ocean (e.g., Smedsrud et al. 2013; Koenigk and Brodeau 2014; Maslowski et al. 2014; Woodgate and Peralta-Ferriz 2021; Zhang et al. 2021). In addition, many of these passages are relatively shallow (e.g., Bering Strait or Barents Sea Opening), and hence E3SM-Arctic has increased its vertical resolution to 80 levels, compared to 60 levels in E3SM-LR.

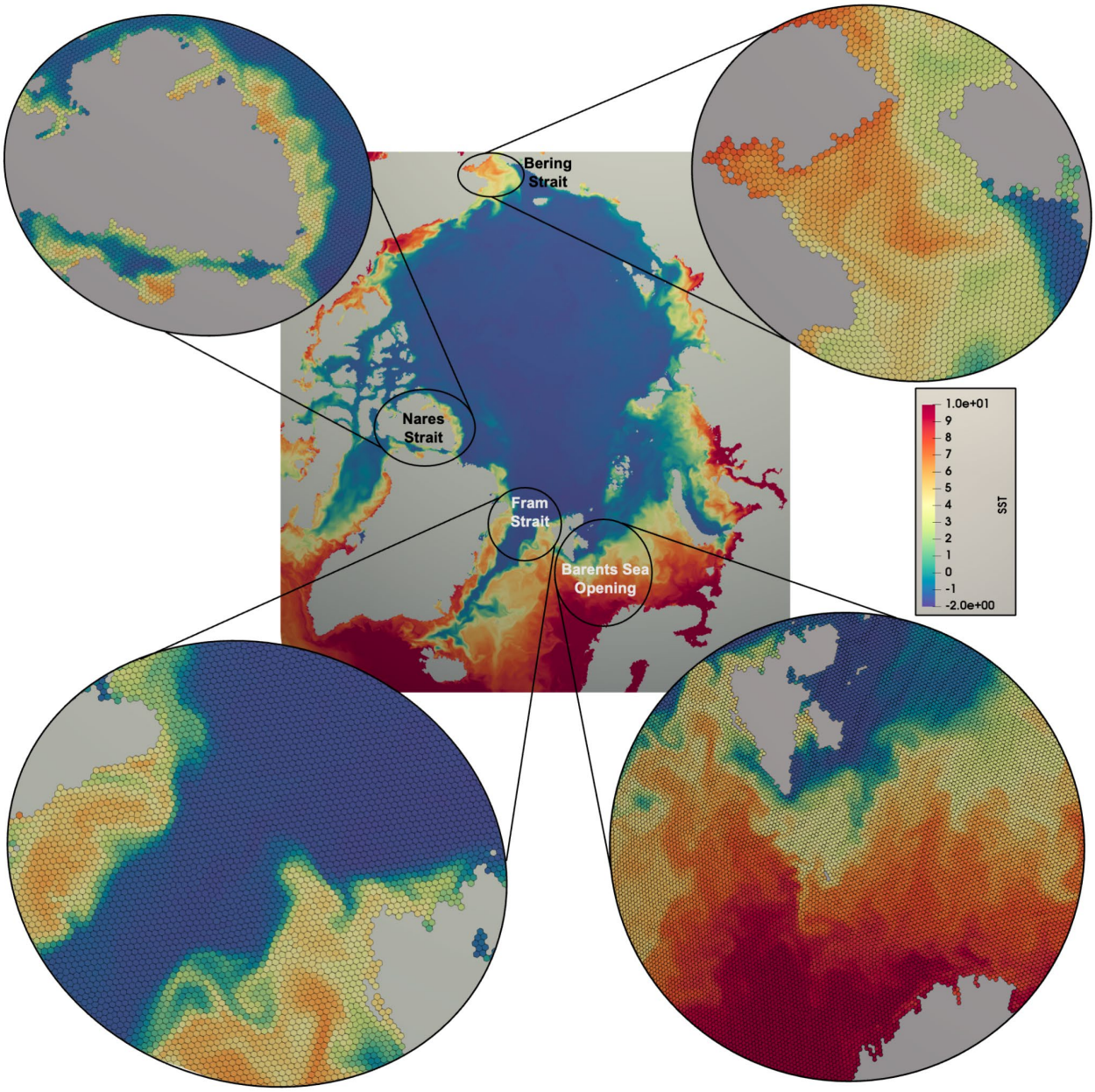

Figure 2. *Zoom-in around the Arctic of a Sea Surface Temperature (SST) field simulated by E3SM-Arctic, with further enlargements at four main gateways (counterclockwise from lower left corner: Fram Strait, Barents Sea Opening, Bering Strait, and Nares Strait), to show the hexagonal mesh and the simulated field in more detail.*

Mesoscale eddy transport in regions outside of the Arctic and pan-Arctic are parameterized using the Gent-McWilliams (GM) parameterization (Gent and McWilliams 1990). We achieve a regionally varying GM by making the GM coefficient dependent on the grid cell size. For the E3SM-Arctic configuration considered here, the GM kappa parameter varies linearly between zero for cell sizes below 20 km and a maximum value of 600 m2/s for cell sizes above 30 km. This implies that we effectively transition from GM-on to GM-off between 10°−28°N in the North Atlantic, and between 25°−50°N in the North Pacific (indicated by the white and red lines in Fig. 1). GM is turned on everywhere in E3SM-LR.

All versions of E3SM used in this study, including E3SM-Arctic, are forced by the Japanese atmospheric reanalysis, spanning the period from 1958 to 2016 (JRA55; Tsujino et al. 2018). We repeated this cycle three times to allow the ocean sufficient time to equilibrate.

3.0 Results

3.1 Global Metrics

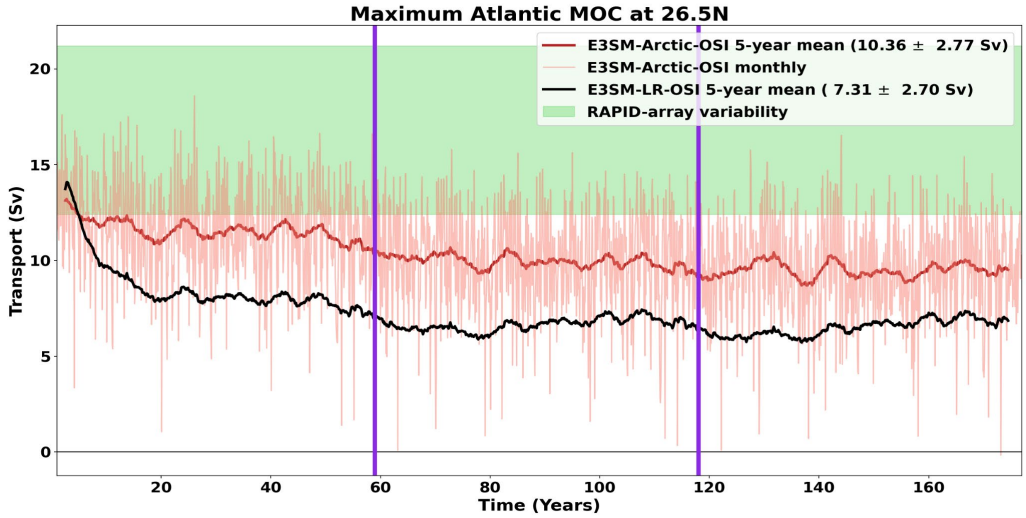

Figure 3. *Time series of the 5-year running average maximum Atlantic MOC at 26.5°N (latitude of the RAPID-MOCHA observational array) from E3SM-Arctic-OSI (dark red line) and E3SM-LR-OSI (black line). The light red line shows E3SM-Arctic-OSI monthly values. The numbers shown in the insets are the mean and standard deviations of the annual model values, computed over the full time series. The RAPID array typical variability (16.8 ± 4.4 Sv) is shaded in green. Finally, the purple vertical lines show the transition across JRA cycles.*

One main benefit of regionally-refined grids is the ability to resolve, or improve representation of, critical physical processes in regions of interest while maintaining a global context for simulations. The first test is to demonstrate that the grid refinement does not deteriorate the solutions in the non-refined regions of the ocean. One of the key metrics of the global ocean circulation is the strength of the Atlantic Meridional Overturning Circulation (AMOC). Standard-resolution configurations of E3SM typically display a weak AMOC compared to observations (e.g., Petersen et al. 2019), and E3SM-LR-OSI is no exception with an AMOC strength of only 7.3 Sv (Fig. 3). The AMOC in E3SM-Arctic-OSI is 10.4 Sv (i.e., 42% stronger), so the grid refinement in the North Atlantic has partly alleviated the weak AMOC bias.

The improved representation of the AMOC is likely associated with improvements in convection processes in the subpolar North Atlantic. Figure 4 shows an example of monthly mean Mixed Layer Depth (MLD), illustrating i) the generally intensified winter convection simulated in E3SM-Arctic-OSI in the Greenland, Irminger, and Labrador Seas – regions important for North Atlantic Deep Water formation – and ii) the detailed structure and realistic magnitudes of the MLD/convection processes (Piron et al. 2016; Holte et al. 2017; Brakstad et al. 2019) that E3SM-Arctic is able to resolve at these latitudes compared with its low resolution counterpart.

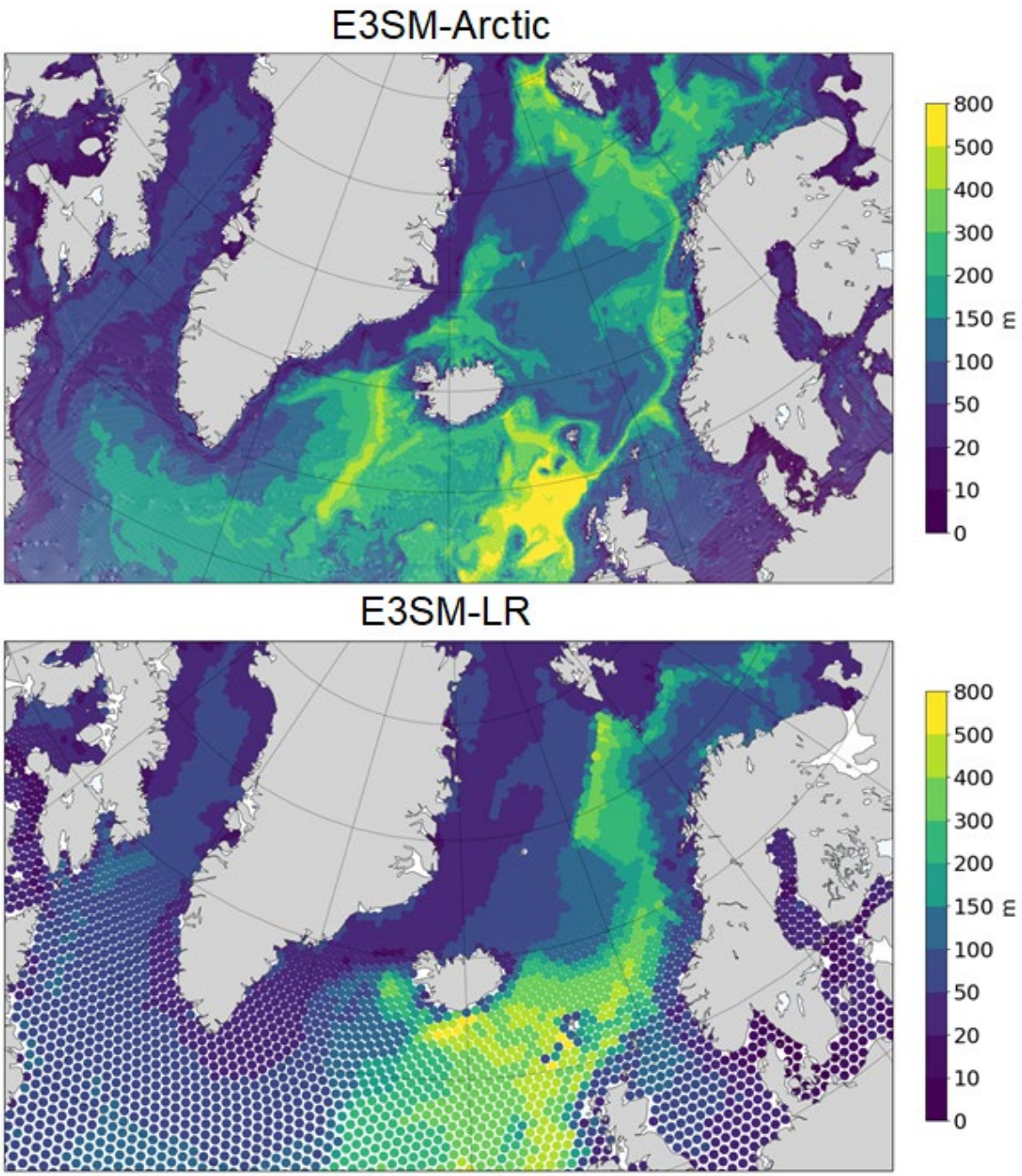

Figure 4. *Monthly mean (February of 2012) mixed layer depth (MLD) simulated in E3SM-Arctic-OSI (upper) and E3SM-LR-OSI (lower). Note the intensified convection in the Greenland, Irminger, and Labrador Seas in E3SM-Arctic compared with its low resolution counterpart, and the detailed circulation structures in this critical region of the World Ocean. MLD fields are plotted as colored circles on their respective native MPAS meshes. In most regions these circles overlap to provide a continuous view of the field, but the lower panel contains regions where the (arbitrary) size of these circles is smaller than the grid spacing.*

3.2 Ocean Gateway Transports and Arctic Stratification

Figures 5 and 6 compare the volume and heat transports in E3SM-Arctic and E3SM-LR through two of the main gateways between the North Atlantic and Arctic Oceans, namely the Barents Sea Opening (BSO) and the Fram Strait. Observational estimates, shaded in green, remain uncertain due to their limited coverage in space and time (Beszczynska-Möller et al. 2011; Smedsrud et al. 2013). The red bars in these plots show estimates from ocean reanalyses, which provide estimates of the ocean state that are consistent both with available observations and dynamical constraints (Uotila et al. 2019). Volume transport through the BSO in E3SM-Arctic is significantly stronger than in E3SM-LR, and consistent with the reanalysis products, which estimate stronger fluxes than what is inferred from the limited observations alone. The volume transport through the Fram Strait is quite comparable between E3SM-Arctic and E3SM-LR, and generally consistent with the observations and reanalysis products. However, heat transports through both BSO and Fram Strait are significantly stronger in E3SM-Arctic than in E3SM-LR, and more consistent with observational and reanalysis estimates. This is a consequence of the E3SM-Arctic ability to represent the complex current and frontal structures in these straits much more accurately than E3SM-LR, as shown in Fig. 7 for the Fram Strait. Heat supply to the Arctic from the lower latitudes is an important driver of the Arctic heat budget, so the regional refinement has provided a critical improvement for studies of Arctic Amplification.

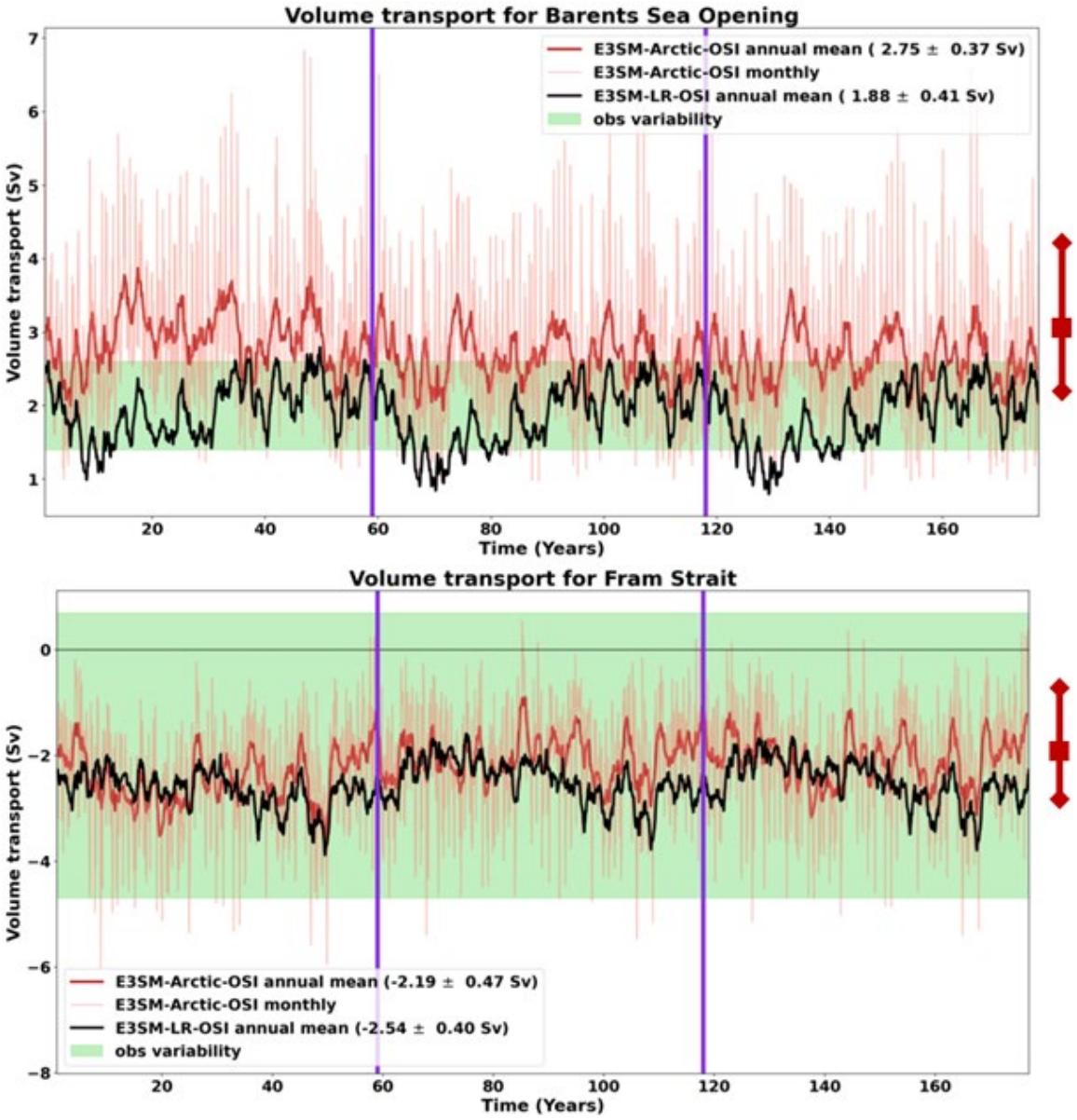

Figure 5. *Time series of annually-averaged volume transport through the (upper) Barents Sea Opening and (lower) Fram Strait, two of the four Arctic gateways shown in Figure 2. E3SM-Arctic-OSI is shown in red and E3SM-LR-OSI in black. Monthly values for E3SM-Arctic-OSI are shown in light red but omitted for E3SM-LR-OSI for clarity. The numbers shown in the insets are the mean and standard deviations of the annual model values, computed over the full time series. Observational ranges are shaded in green, while the red bars show the ensemble-mean and range of 10 ocean reanalysis products (Uotila et al. 2019).*

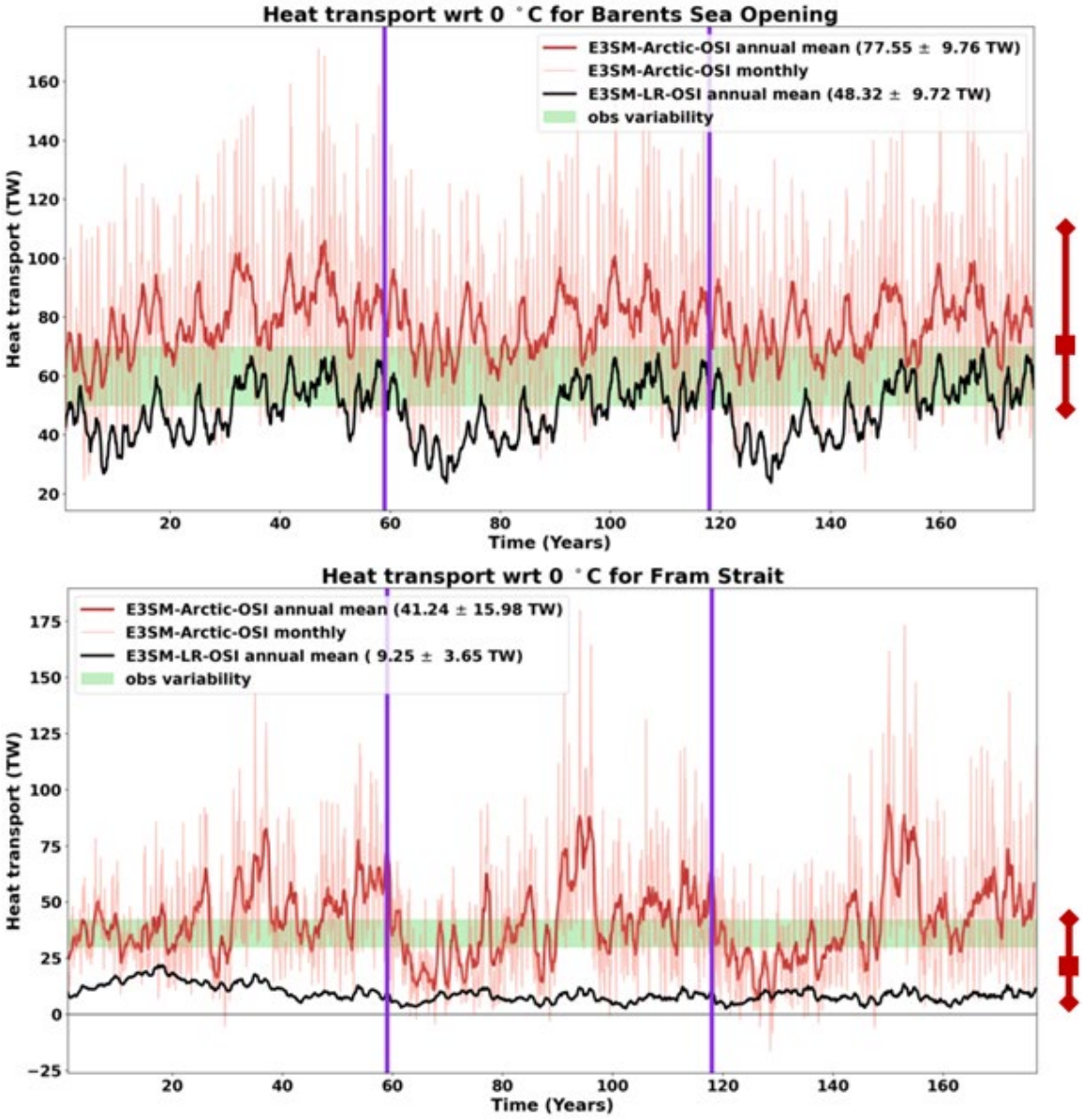

Figure 6. *Similar to Figure 5, but for heat transport.*

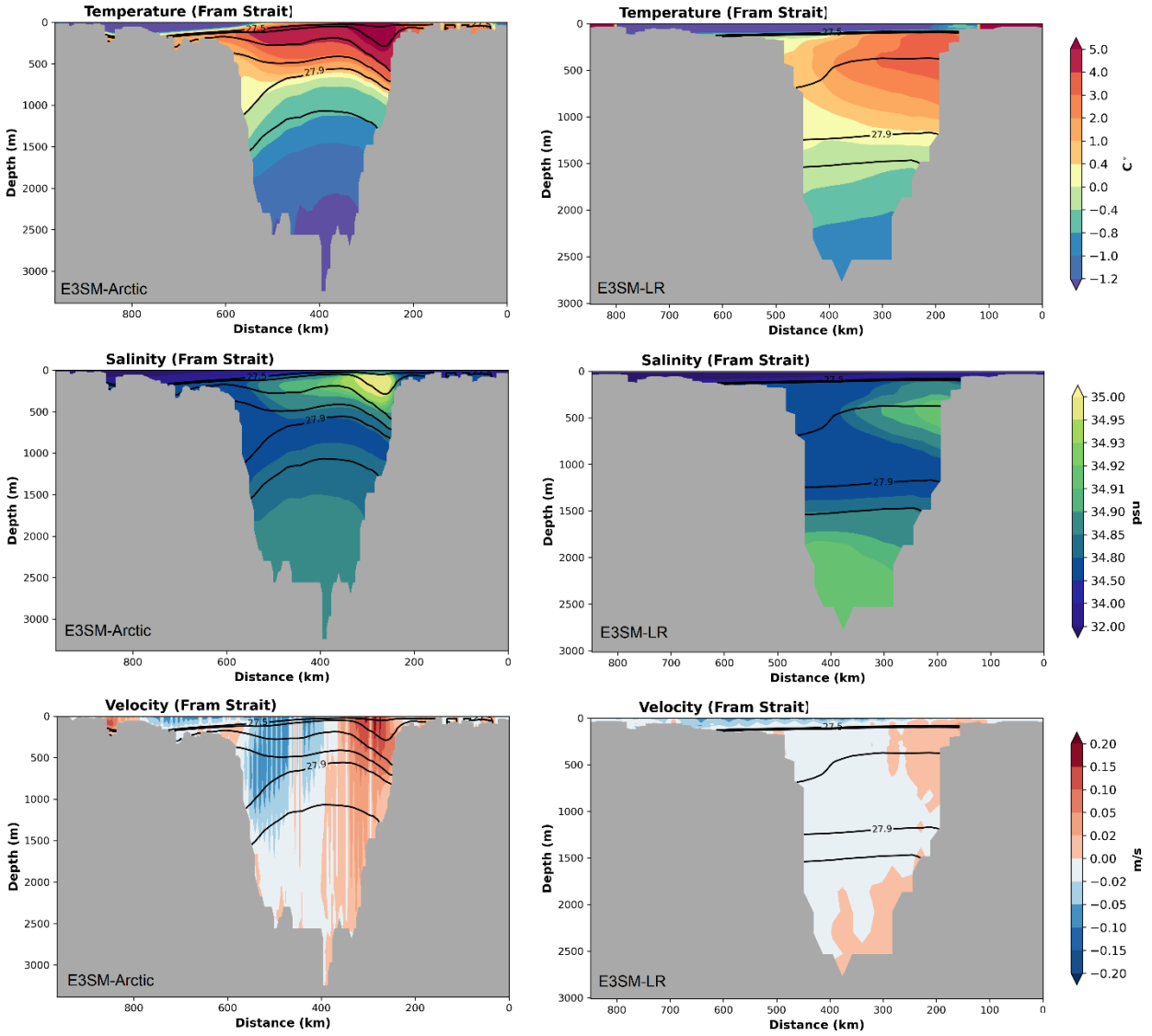

Figure 7. *Cross-section of potential temperature (upper panels), salinity (middle panels), and normal velocity (bottom panels) for the Fram Strait, for E3SM-Arctic-OSI (left panels) and E3SM-LR-OSI (right panels). Annual climatologies are computed over years 166-177. Black contours show potential density. Note unrealistic fresh upper ocean and excessively broad and weakened Atlantic Water inflow in E3SM-LR.*

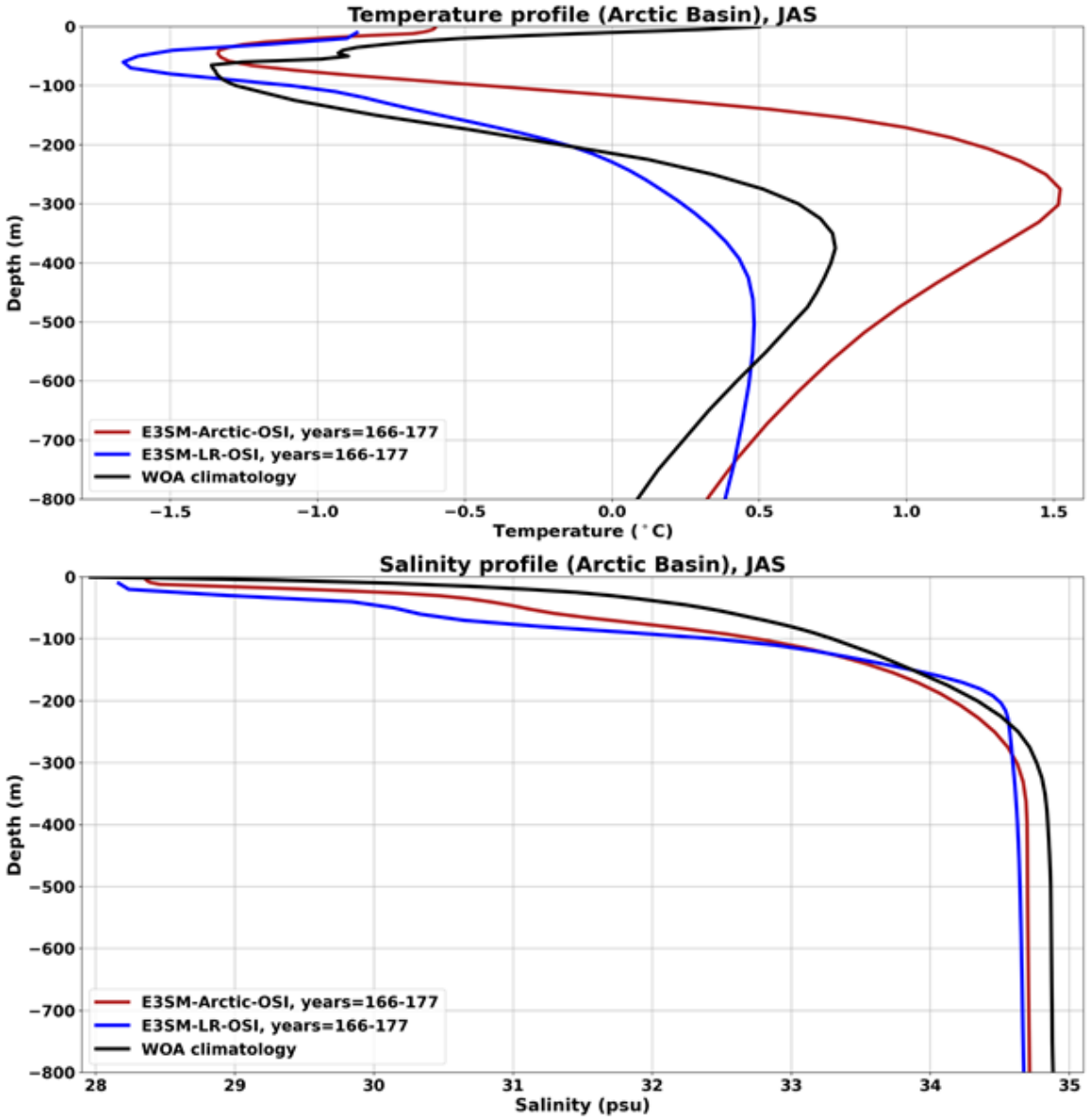

Figure 8. *Averaged temperature (upper) and salinity (lower) profiles for the Arctic Basin for a climatological summer season (July-August-September) computed over the last 12 years of the third JRA55 cycle (2005-2016). Results for E3SM-Arctic-OSI and E3SM-LR-OSI are shown in red and blue, respectively, whereas WOA climatology is shown in black. Note that differences between model and WOA, both in terms of biases and vertical structure, are generally reduced in E3SM-Arctic compared to E3SM-LR, especially in terms of the representation of Atlantic Water below 100 m depth, and of the halocline below 50 m.*

Grid refinement has also improved the stratification in the Arctic (Fig. 8). Of particular importance is the representation of the Atlantic layer, a layer of warm and salty waters below 100 m depth that enter the Arctic through the BSO and Fram Strait. The fact that E3SM-Arctic simulates a distinct subsurface temperature maximum -despite being too warm and shallow- is a great improvement over E3SM-LR, which does not reproduce the Atlantic Layer at all.

3.3 Sea Ice

Sea ice thickness and area are important metrics, which result from dynamical and thermodynamical processes within the sea ice as well as its interaction with the atmosphere above and the ocean below. One of the key dynamical processes commonly under-represented in low-resolution sea ice models (Kwok et al. 2008) is sea ice deformation, including divergence, shear and vorticity, which impact deformation-related ice production. Figure 9 shows the comparison of monthly mean sea ice divergence and shear between the E3SM-Arctic-OSI and E3SM-LR-OSI simulations for the month of June 2012. Comparison of modeled sea ice deformations to those derived from the RADARSAT Geophysical Processor System (RGPS) by Kwok et al. (2008) showed that regional divergence and shear of the ice cover is commonly under-estimated. The higher resolution of the E3SM-Arctic-OSI indeed allows both more realistic representation of the linear kinematic features (LKF) observed from satellites as well as larger magnitudes and aerial coverage of divergence and shear compared to the diffusive fields simulated in E3SM-LR-OSI.

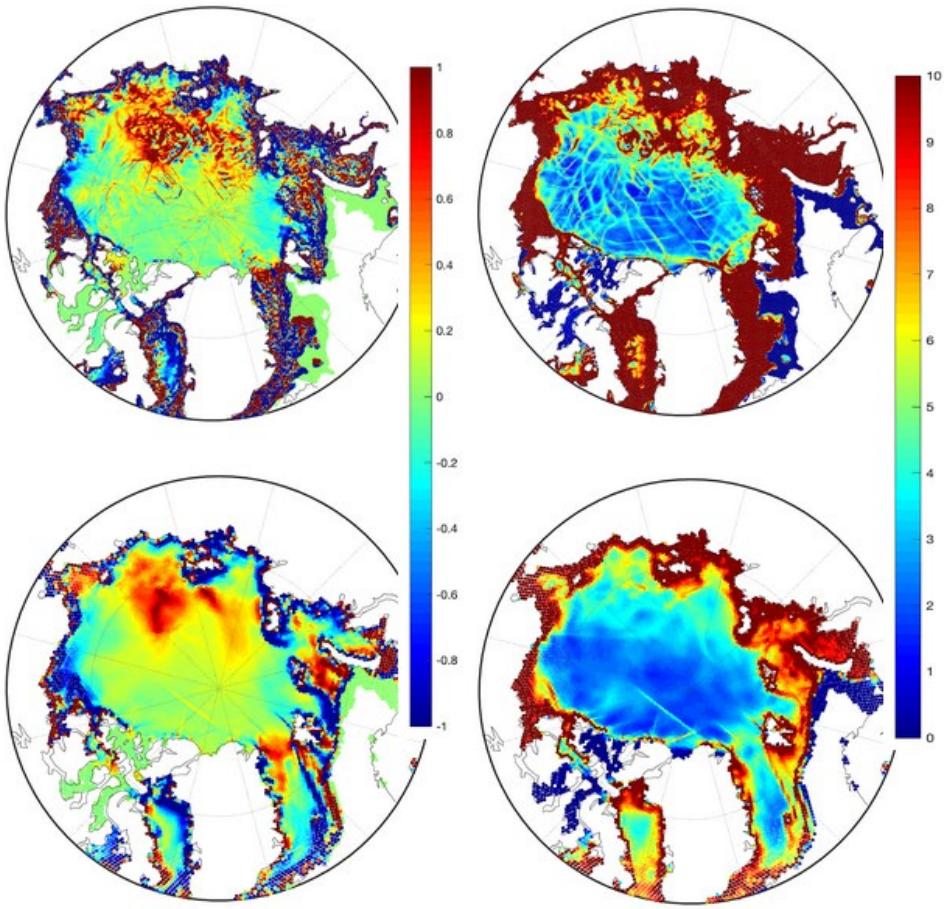

Figure 9. *Monthly mean sea ice divergence (left; %/day) and shear (right, %/day) from E3SM-Arctic-OSI (top) and E3SM-LR-OSI (bottom) for June 2012. The so-called 'linear kinematic features' or LKFs, commonly observed by satellites (Kwok et al. 2008), are more realistically simulated in the Arctic-refined model configuration.*

Other key metrics of Arctic sea ice benefit less from enhanced spatial resolution in E3SM-Arctic compared to E3SM-LR. For instance, both configurations have too thick sea ice in the Amerasian Basin (Pacific side), and too thin sea ice in the Eurasian Basin, as shown in Fig. 10. These biases, especially in

E3SM-Arctic-OSI, are likely due to sub-optimal parameter settings that point to the need for further tuning or a consequence of known biases in the atmospheric reanalyses used to force these models (Batrak and Müller 2019).

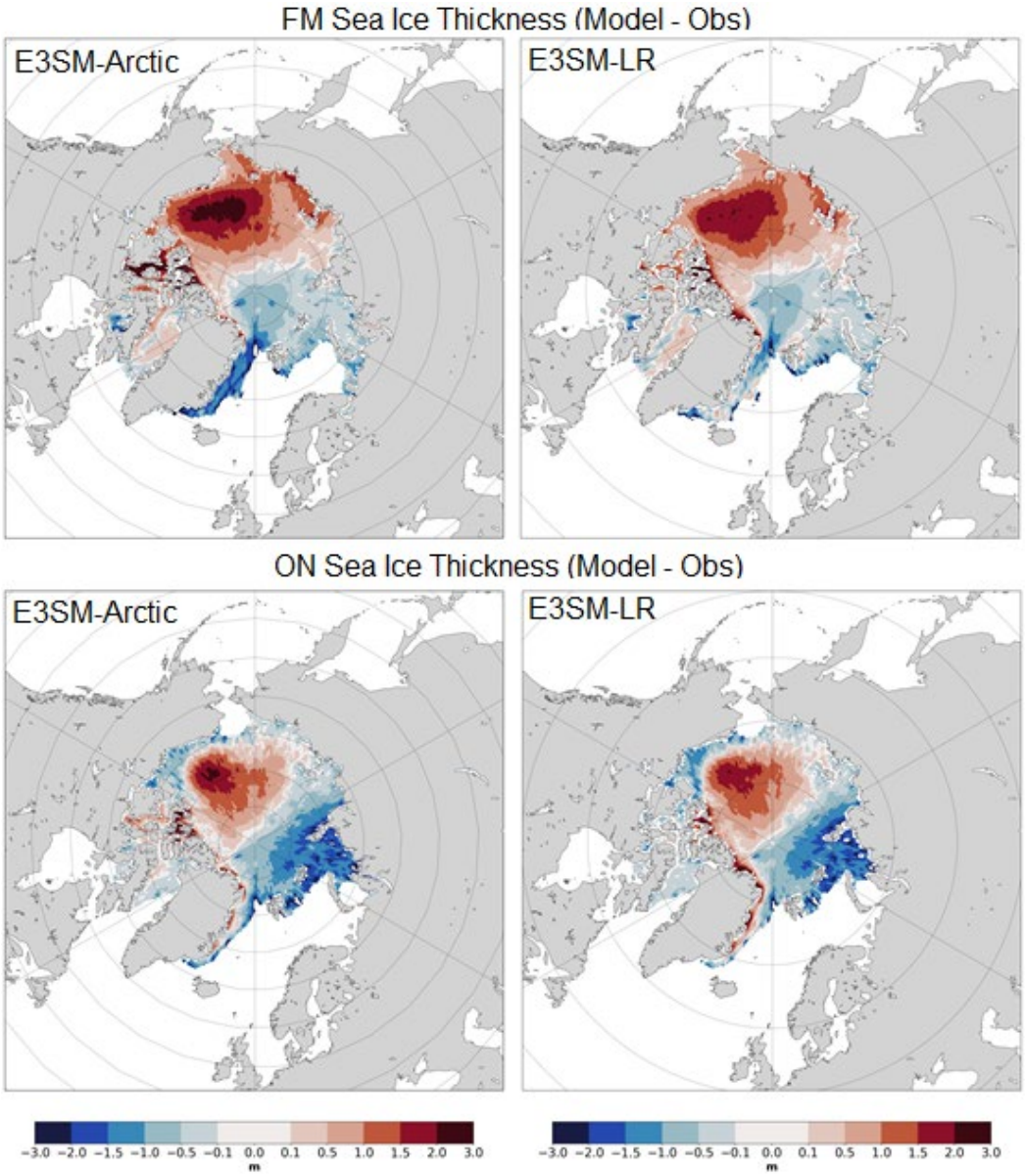

Figure 10. *February-March (FM; top panels) and October-November (ON; bottom panels) climatology of the sea ice thickness bias for (left) E3SM-Arctic-OSI and (right) E3SM-LR-OSI, with respect to a climatology based on IceSat observations from 2003 to 2009. The model climatology is computed over model years 166-177 (2005-2016).*

We are continuing our development and experimentation with E3SM-Arctic using the E3SMv2 code base. In particular, we are tuning the model with a specific focus on reducing the sea ice thickness bias. Figure 11 shows Arctic-integrated sea ice volume for several different simulations, compared with the PIOMAS (Zhang et al. 2003, Schweiger et al. 2011) reanalysis product (green dashed). The red curve shows a significant sensitivity and improvement of the Arctic sea ice volume with respect to a change of

the parameter Cf, which is a scaling factor relating the work against gravity to the work against friction during ridging to determine the effective energy dissipation rate (Rothrock 1975). Figure 12 shows the sea ice thickness distribution from the default 60to10 configuration and from the configuration with the modified Cf parameter after 15 years of integration, clearly demonstrating an improvement due to the reduced sea ice thickness in the central Arctic, comparable to the limited ice thickness measurements from submarines for a similar period (see Figure 1 in Kwok and Rothrock 2009). Other parameter sensitivity simulations are underway to further tune the E3SM-Arctic configuration, especially with respect to its representation of sea ice thickness distribution.

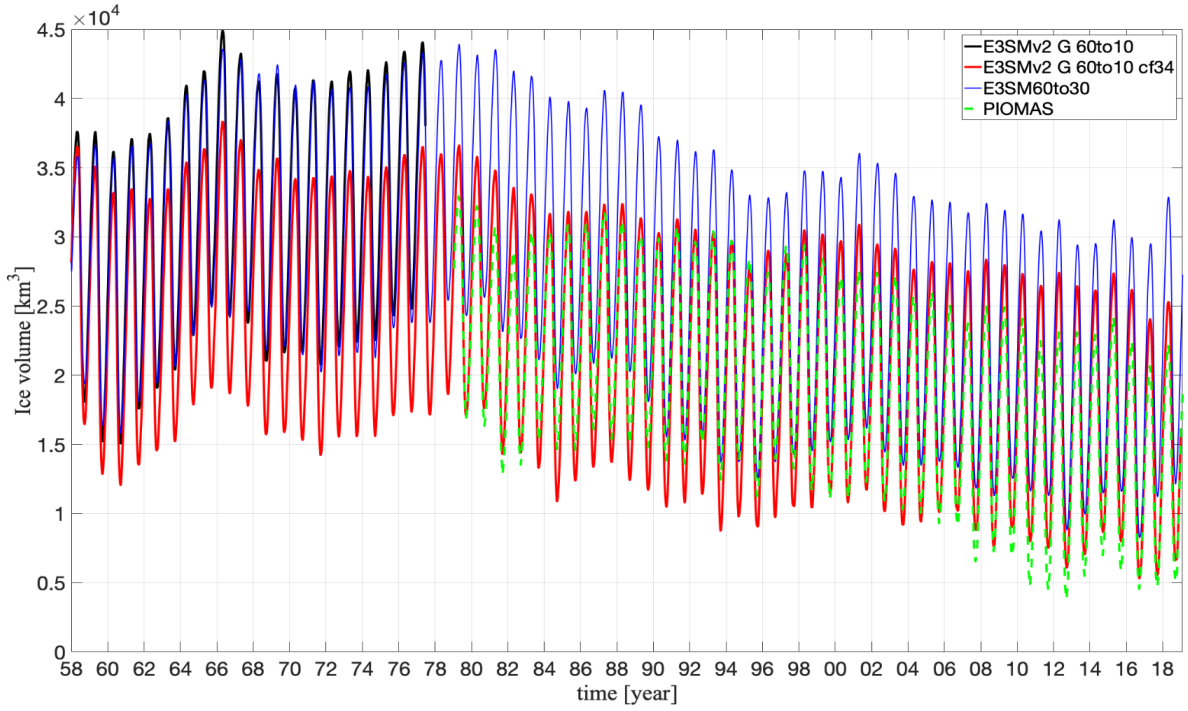

Figure 11. *Time series of sea ice volume from the 60to10 cf34 experiment (red line) relative to the reference 60to10 integration (black line), 60to30 (blue line), and PIOMAS reanalysis (dashed green line). Note that the 60to30 run is E3SMv1, whereas the 60to10 results are from E3SMv2.*

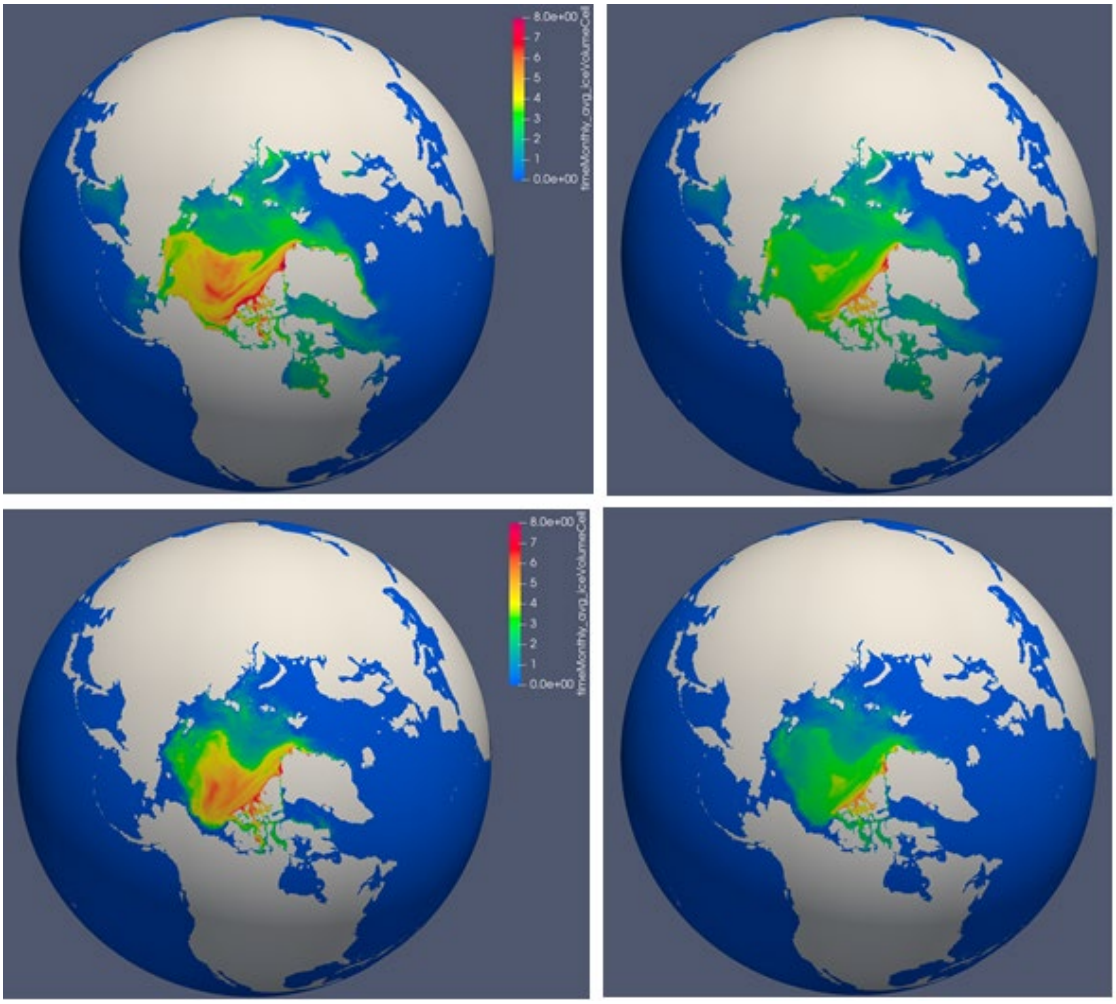

Figure 12. *Maps of sea ice thickness distributions from the default (left) and cf34 (right) experiments in March (top) and September (bottom) after 15 years of integration. Increasing the value of the parameter Cf as part of our tuning activity has reduced the sea ice thickness and reduced the bias shown in Fig. 10.*

To conclude, we have demonstrated that the Arctic-refined configuration of E3SM, with grid resolution of 10 km in the North Atlantic and Arctic Oceans, provides significant improvements in the representation of features that are important for the Arctic Ocean and its interactions with lower latitudes, including the strength of the AMOC; heat transport into the Arctic; the stratification of the Arctic and the representation of the Atlantic Water layer; and sea ice deformation. In the current forced ocean-sea ice coupled simulations sea ice thickness distributions are not improved, as sea ice conditions are primarily controlled by atmospheric forcing. We anticipate seeing more significant improvements in the fully-coupled simulations, where ocean-atmosphere-sea ice feedbacks are likely to amplify the differences induced by a more detailed representation of the ice pack (for instance, leads).

4.0 Contributors to this Report

Wilbert Weijer, Los Alamos National Laboratory
Wieslaw Maslowski, Naval Postgraduate School
Milena Veneziani, Los Alamos National Laboratory

5.0 References

Batrak, Y., & Müller, M. (2019). On the warm bias in atmospheric reanalyses induced by the missing snow over Arctic sea-ice. *Nature communications*, 10(1), 1-8.

Beszczynska-Möller, A., Woodgate, R. A., Lee, C., Melling, H., & Karcher, M. (2011). A synthesis of exchanges through the main oceanic gateways to the Arctic Ocean. *Oceanography*, 24(3), 82-99.

Brakstad, A., Våge, K., Håvik, L., & Moore, G. W. K. (2019). Water Mass Transformation in the Greenland Sea during the Period 1986–2016, *Journal of Physical Oceanography*, 49(1), 121-140.

Gent, P. R., & McWilliams, J. C. (1990). Isopycnal mixing in ocean circulation models. *Journal of Physical Oceanography*, 20(1), 150-155.

Golaz, J. C., Caldwell, P. M., Van Roekel, L. P., Petersen, M. R., Tang, Q., Wolfe, J. D., ... & Zhu, Q. (2019). The DOE E3SM coupled model version 1: Overview and evaluation at standard resolution. *Journal of Advances in Modeling Earth Systems*, 11(7), 2089-2129.

Holte, J., Talley, L. D., Gilson, J., and Roemmich, D. (2017), An Argo mixed layer climatology and database, *Geophys. Res. Lett*., 44, 5618– 5626, doi:10.1002/2017GL073426.

Koenigk, T., & Brodeau, L. (2014). Ocean heat transport into the Arctic in the twentieth and twenty-first century in EC-Earth. *Climate Dynamics*, 42(11), 3101-3120.

Kwok, R., Hunke, E. C., Maslowski, W., Menemenlis, D., & Zhang, J. (2008). Variability of sea ice simulations assessed with RGPS kinematics. *Journal of Geophysical Research: Oceans*, 113(C11).

Kwok, R., & Rothrock, D. A. (2009). Decline in Arctic sea ice thickness from submarine and ICESat records: 1958–2008. *Geophysical Research Letters*, 36(15).

Maslowski, W., Clement Kinney, J., Okkonen, S.R., Osinski, R., Roberts, A.F., Williams, W.J. (2014). The Large Scale Ocean Circulation and Physical Processes Controlling Pacific-Arctic Interactions. In: Grebmeier, J., Maslowski, W. (eds) The Pacific Arctic Region. Springer, Dordrecht.

Nurser, A. J. G., & Bacon, S. (2014). The rossby radius in the arctic ocean. *Ocean Science*, 10(6), 967-975.

Petersen, M. R., Asay-Davis, X. S., Berres, A. S., Chen, Q., Feige, N., Hoffman, M. J., ... & Woodring, J. L. (2019). An evaluation of the ocean and sea ice climate of E3SM using MPAS and interannual CORE-II forcing. *Journal of Advances in Modeling Earth Systems*, 11(5), 1438-1458.

Piron, A., Thierry, V., Mercier, H., & Caniaux, G. (2016). Argo float observations of basin-scale deep convection in the Irminger sea during winter 2011–2012. Deep Sea Research Part I: *Oceanographic Research Papers*, 109, 76-90.

Rothrock, D. A. (1975). The energetics of the plastic deformation of pack ice by ridging. *Journal of Geophysical Research*, 80(33), 4514-4519.

Schweiger, A., Lindsay, R., Zhang, J., Steele, M., Stern, H., & Kwok, R. (2011). Uncertainty in modeled Arctic sea ice volume. *Journal of Geophysical Research: Oceans*, 116(C8).

Smedsrud, L. H., Esau, I., Ingvaldsen, R. B., Eldevik, T., Haugan, P. M., Li, C., ... & Sorokina, S. A. (2013). The role of the Barents Sea in the Arctic climate system. *Reviews of Geophysics*, 51(3), 415-449.

Tsujino, H., Urakawa, S., Nakano, H., Small, R. J., Kim, W. M., Yeager, S. G., ... & Yamazaki, D. (2018). JRA-55 based surface dataset for driving ocean–sea-ice models (JRA55-do). *Ocean Modelling*, 130, 79-139.

Uotila, P., Goosse, H., Haines, K., Chevallier, M., Barthélemy, A., Bricaud, C., ... & Zhang, Z. (2019). An assessment of ten ocean reanalyses in the polar regions. *Climate Dynamics*, 52(3), 1613-1650.

Veneziani, M., W. Maslowski, Y. Lee, G. D'Angelo, R. Osinski, M. Petersen, W. Weijer, T. Craig, J. Wolfe, D. Comeau, A. Turner: An evaluation of the E3SM-Arctic Ocean/Sea Ice Regionally Refined Model. *Geoscientific Model Development*, in press.

A Woodgate, R., & Peralta-Ferriz, C. (2021). Warming and Freshening of the Pacific Inflow to the Arctic from 1990-2019 implying dramatic shoaling in Pacific Winter Water ventilation of the Arctic water column. *Geophysical Research Letters*, 48(9), e2021GL092528.

Zhang, J., Weijer, W., Steele, M., Cheng, W., Verma, T., & Veneziani, M. (2021). Labrador Sea freshening linked to Beaufort Gyre freshwater release. *Nature communications*, 12(1), 1-8.

Zhang, J., & Rothrock, D. A. (2003). Modeling global sea ice with a thickness and enthalpy distribution model in generalized curvilinear coordinates. *Monthly Weather Review*, 131(5), 845-861.

U.S. DEPARTMENT OF
ENERGY

Office of Science